

A HEAT PUMP MODEL FOR HEAT PUMP DRYING STUDY

Dr.Somnuk Theerakulpisut Professor W.W.S. Charters

Assistant Professor

Dean of Engineering

Khon Kaen University

The University of Melbourne

Khon Kaen 40002

Australia

ABSTRACT

Drying is a common process in a number of industries. In practice, much of the commercial drying plant is not energy efficient for various reasons, one of which is that commercially available dryers are not generally equipped with heat recovery facilities. With heat pumps, however, it is possible to recover both sensible and latent heat and to use to best advantage the high grade energy input to the heat pump compressor.

Because of the inherent system complexity, it is important to formulate accurate simulation models of the heat pump and of the drying process and to combine them into a single-system model for dryer performance evaluation.

In this paper, a brief coverage is given of the development of the heat pump model for combining with a fixed-bed drying model to form a range of heat pump dryer configurations which may be used to study the heat pump dryer configurations of interest. Modelling approaches, equations and computational procedures for system component models are also described.

แบบจำลองของฮีทปั๊มสำหรับการศึกษาระบบอบแห้งโดยฮีทปั๊ม

บทคัดย่อ

บทความนี้อธิบายถึงการสร้างแบบจำลองทางคณิตศาสตร์ของฮีทปั๊มเพื่อใช้ในการศึกษาระบบอบแห้งเนื่องจาก ระบบอบแห้งโดยฮีทปั๊มเป็นระบบที่มีความซับซ้อนเนื่องจากขบวนการถ่ายเทความร้อนและมวลที่เกิดขึ้นจึงมีความจำเป็นที่จะต้องมีการสร้างแบบจำลองทางคณิตศาสตร์ที่แม่นยำของฮีทปั๊มซึ่งสามารถนำไปรวมกับแบบจำลองของการอบแห้งเพื่อนำไปศึกษาระบบอบแห้งโดยฮีทปั๊มแบบต่าง ๆ ได้บทความนี้ได้กล่าวถึงเฉพาะแบบจำลองของฮีทปั๊มเท่านั้นโดยอธิบายถึงวิธีการสร้างแบบจำลอง สมการต่าง ๆ และขั้นตอนการคำนวณของแบบจำลองย่อยของชิ้นส่วนของระบบแบบจำลองของฮีทปั๊มที่ได้พัฒนาขึ้นมาซึ่งได้รับการทดสอบกับข้อมูลการทดลองแล้ว และพบว่าแบบจำลองมีความแม่นยำสูงและเหมาะที่จะนำไปใช้ในการศึกษาในระบบอบแห้งโดยฮีทปั๊มต่อไป

INTRODUCTION

In the usual approach to modelling heat pumps or other complex thermal systems, attempts are made to characterize the numerous processes occurring within the system by

means of algebraic equations or possible ordinary differential equations. Even within this framework, a broad range of models is possible, depending on the generality and accuracy required. The size and complexity of the model are influenced by the level of detail with which each component is modelled, the degree of empiricism employed, and the simplifying assumptions used.

In this study, heat pump component models will be developed by making use of the specific characteristics of the heat pump components. Empirical equations will be employed to describe heat and/or mass transfer on the refrigerant and air sides. Single-phase and two-phase pressure drop correlations will be used to take account of pressure drops occurring in the heat pump components. Properties of moist air and refrigerant will also be modelled. The benefit from such a detailed modelling technique is expected to be in a highly accurate heat pump model to serve the heat pump drying study.

HEAT PUMP MODEL

Figure 1 shows a pressure-enthalpy diagram representing a single-stage vapour compression heat pump cycle. The cycle deviates from the theoretical cycle in several respects. Pressure drops in compressor suction and discharge valves are assumed. Heat gains in the compressor suction line and heat losses in the compressor discharge line and the condenser liquid line are also assumed. Pressure drops in the evaporator, condenser and piping are taken into account. The compression process is assumed to be polytropic.

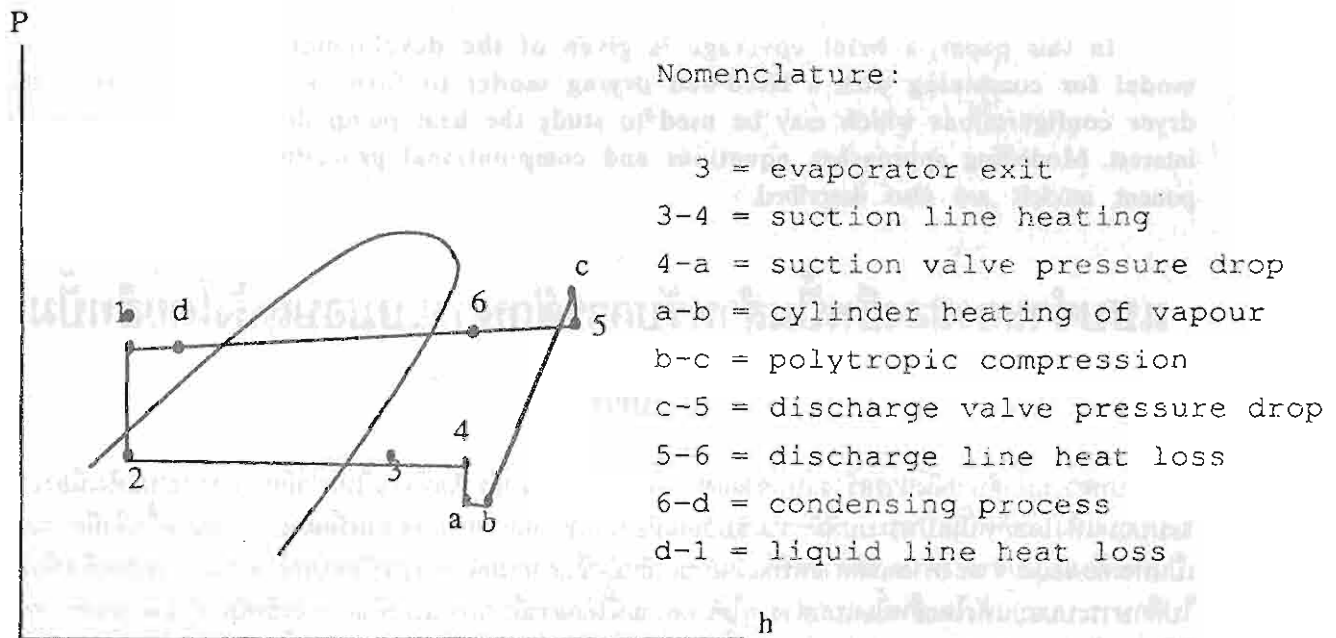


Figure 1: Pressure-enthalpy diagram of a practical heat

The heat pump to be modelled in this study is based on this cycle. The model will require the specifications of evaporator superheat, evaporator and condenser inlet air conditions, and dimensions of components and interconnecting pipes. Without delving into details of the simulation procedure of the model, the calculational scheme will be briefly outlined. With reference to Figure 1, simulation starts with an initial estimate of P_3 and the specified degrees of superheat to fix state (3). State (4) is then fixed by calculating heat

gain by the suction line assuming negligible pressure drop in the line. By estimating the pressure drop across the compressor suction valve and cylinder heating effect, state (b) is established. The compressor model is then used to predict P4 and the compressor work input which give h_c , hence state (c) is fixed. State (5) fixed by assuming the pressure drop and isentropic process across the discharge valve. State (6) is then established from the discharge line model. With the knowledge of inlet air condition to the condenser and refrigerant state (6), the condenser model is used to calculate state (d) and air condition at the condenser exit. State(d) is then used in the liquid line model to calculate state (1). Once state (1) is known, the high-pressure side is established.

The next task is the low-pressure side analysis. From the knowledge of refrigerant state (3) and by assuming evaporator inlet air condition, the evaporator model is used in a backward computational scheme to calculate refrigerant state (2). The enthalpy at this state, h_2 , is compared with the enthalpy at the inlet of the thermostatic expansion valve, h_1 . If they do not agree within a specified limit, the evaporator inlet air temperature is varied until the agreement is achieved. When h_1 and h_2 agree within a specified tolerance, a system solution has been completed for some evaporator inlet air temperature. This inlet air temperature is then compared with the actual value. If they do not agree within a given limit, the refrigerant pressure at state (3) is changed to a new value, and the whole calculational procedure is repeated until the calculated evaporator inlet air temperature agrees with the actual value.

CONDENSER MODEL

The condenser model is simpler to model than the evaporator because of the absence of dehumidification of water vapour on the condenser coil. The finned-tube condenser surface is divided into desuperheating, two-phase and subcooling zones as shown in Figure 2. These zones of the condenser must be modelled separately. By determining the fractions of the three zones, the heat transfer rate from each section may be computed, and so may the condition of air at the exit of each section. Without going into the details of the modelling procedure, the governing equations for the condenser are listed as follows.

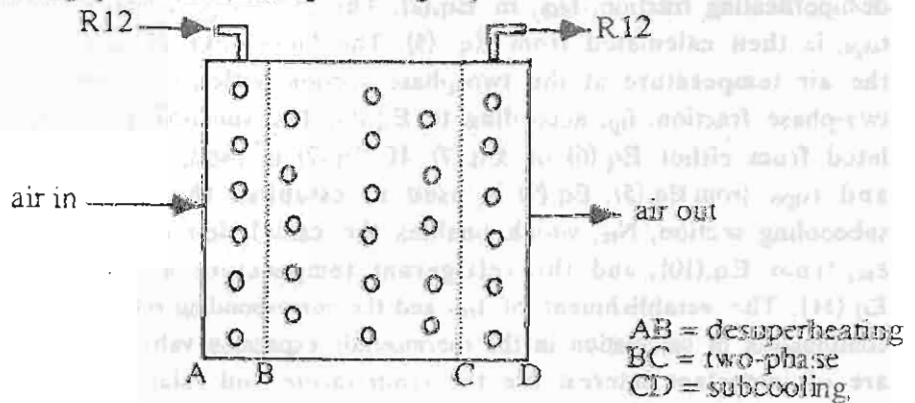


Figure 2 Condenser schematic

$$\frac{C_{rdsh}(t_{rci}-t_{rs})}{C_{min}(t_{rci}-t_{aci})} = 1 - \exp\{N^{0.22}[\exp(-CN^{0.78})-1]/C\} \quad (1)$$

$$N_{dsh} = U_{dsh}A_{dsh}/C_{min} = U_{dsh}f_{dsh}A_c/C_{min} \quad (2)$$

$$t_{atpi} = t_{aci} + C_r(t_{rci}-t_{rs})/C_a \quad (3)$$

$$t_{atpo} = t_{atpi} + m_r h_{fg} / C_a \quad (4)$$

$$f_{tp} = \frac{C_a / U_{tp} A \ln(t_{rs} - t_{atpi})}{(t_{rs} - t_{atpo})} \quad (5)$$

$$f_{sc} = 1 - (f_{tp} + f_{dsh}), \quad \text{for } f_{tp} + f_{dsh} \leq 1 \quad (6)$$

$$f_{sc} = 0, \quad \text{for } f_{tp} + f_{dsh} > 1 \quad (7)$$

$$f_{tp} = 1 - f_{dsh} \quad (8)$$

$$N_{sc} = U_{sc} A_{sc} / C_{min} = U_{sc} f_{sc} A_c / C_{min} \quad (9)$$

$$\epsilon_{sc} = 1 - \exp\{N^{0.22} [\exp(-CN^{0.78}) - 1] / C\} \quad (10)$$

$$t_{rco} = t_{rs} - \epsilon_{sc} C_{min} (t_{rs} - t_{atpo}) / C_{rsc} \quad (11)$$

$$t_{aco} = t_a + q_c / C_a \quad (12)$$

$$q_c = C_{rdsh} (t_{rci} - t_{rs}) + C_a (t_{atpo} - t_{atpi}) + C_{rsc} (t_{rs} - t_{rco}) \quad (13)$$

$$U = \frac{1}{\frac{A_c}{A_{ti} b_i} + \frac{(1-\phi)}{h_o (A_{to}/A_f + \phi)} + \frac{1}{h_o}} \quad (14)$$

Eq.(1) is obtained using the definition of heat exchanger effectiveness and the effectiveness-NTU relationship, as given in Kreider and Kreith [1], for a cross-flow heat exchanger with both fluids unmixed. The equation is iteratively solved for the number of transfer units for the desuperheating section, N_{dsh} , which is, in turn, used to solve for the desuperheating fraction, f_{dsh} , in Eq.(2). The air temperature at the two-phase section inlet, t_{atpi} , is then calculated from Eq. (3). The knowledge of t_{atpi} is used in Eq. (4) to compute the air temperature at the two-phase section outlet, t_{atpo} , which is used to establish the two-phase fraction, f_{tp} , according to Eq.(5). The subcooling fraction, f_{sc} , may now be calculated from either Eq.(6) or Eq.(7). If Eq.(7) is used, f_{tp} , must be calculated from Eq.(8), and t_{atpo} from Eq.(5). Eq.(9) is used to establish the number of transfer units for the subcooling section, N_{sc} , which enables the calculation of the heat exchanger effectiveness, ϵ_{sc} , from Eq.(10), and the refrigerant temperature at the condenser outlet, t_{rco} , from Eq.(11). The establishment of t_{rco} and the corresponding refrigerant pressure is important for the continuation of calculation in the thermostatic expansion valve model to be later described. What are of important interest are the temperature and relative humidity of the air leaving the condenser since the knowledge of these two parameters is required in the fixed-bed drying model. The air temperature leaving the condenser, t_{aco} , may be calculated from Eq.(12) whereas the air relative humidity at the condenser exit will assume the value of the relative humidity at the condenser inlet since there is no dehumidification of water vapour on the condenser coil. The heating capacity of the heat pump is expressed as the sum of heat transfer in each section of the condenser as in Eq.(13). Eq.(14) describes the general relationship from which the overall heat transfer coefficient for a dry heat exchanger may be calculated.

EVAPORATOR MODEL

An evaporator is used to extract both sensible and latent heat of air, hence the air is cooled. It is common that dehumidification of air also occurs in this process. With dehumidification, the air-side surface is wetted with liquid water or frost. It, therefore, follows that the method generally used in the analysis of dry air-side surface does not suffice.

The main task of the evaporator model in this study is the prediction of the air condition at the evaporator outlet and the refrigerant state at the inlet of the evaporator. The evaporator model may therefore be considered to be working in a backward scheme to predict the refrigerant state at the inlet rather than the outlet.

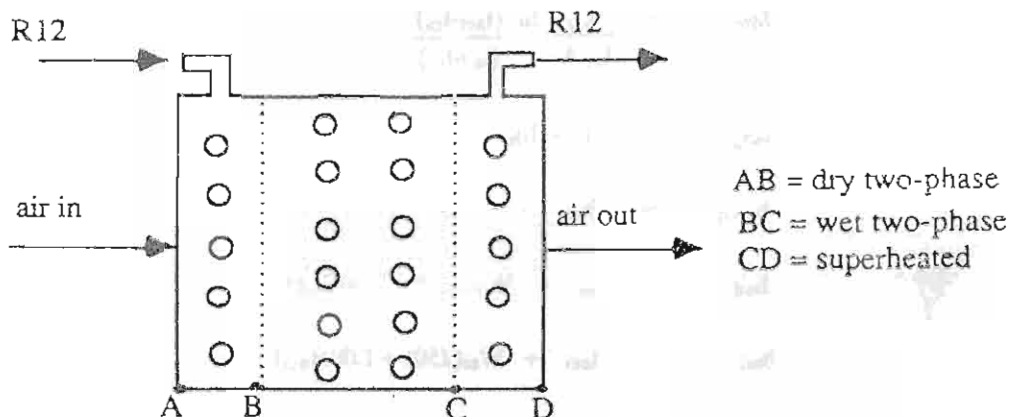


Figure 3 Evaporator schematic

As in the case of the condenser model, the two-phase and superheating fractions of the evaporator must be modelled so that the heat and/or mass transfer in each section may be analyzed. It will be assumed that dehumidification may occur only on the two-phase surface. In reality the two-phase surface may be entirely dry, partially wet or totally wet, depending on the condition of the incoming air. For this reason, the two-phase surface section is further divided into wet and dry two-phase surfaces as indicated in Figure 3.

Since most evaporators generally operate with some wet section, the modelling approach for the entirely dry evaporator will not be discussed in this paper. However, two equations derived for the dry evaporator will be presented for later use. If the evaporator is entirely dry, the heat transfer rate for the two-phase section is given by

$$q_{tp} = m_r(h_{rsv} - h_{rtpi}) \quad (15)$$

and the air temperature at the two-phase section outlet by

$$t_{atpo} = t_{aci} + q_{tp}/C_a \quad (16)$$

The value of t_{atpo} as given by Eq.(16) will be used to compare with the air temperature at the location where dehumidification just begins to determine whether the evaporator operates with some wet surface.

For the evaporator operating with some wet surface, the following equations form the model.

$$\frac{C_r(t_{rsho}-t_{rs})}{C_{min}(t_{atpo}-t_{aei})} = 1 - \exp\{N^{0.22}[\exp(-CN^{0.78})-1]/C\} \quad (17)$$

$$f_{sh} = N_{sh}C_{min}/U_eA_e \quad (18)$$

$$f_{tp} = 1 - f_{sh} \quad (19)$$

$$t_{ad} = \frac{t_d - (1-U_eA_e/h_iA_{ti})t_{rs}}{1 - (1-U_eA_e/h_iA_{ti})} \quad (20)$$

$$f_{dtp} = \frac{C_a \ln(t_{aei}-t_{rs})}{U_eA_e(t_{ad}-t_{rs})} \quad (21)$$

$$f_{wtp} = 1 - f_{sh} - f_{dtp} \quad (22)$$

$$h_{awtpo} = h_{asr} + (h_{ad}-h_{asr})\exp(-U_wf_{wtp}A_e/m_a) \quad (23)$$

$$h_{ad} = t_{ad} + W_{ei}(2501 + 1.085t_{ad}) \quad (24)$$

$$h_{aei} = t_{aei} + W_{ei}(2501 + 1.085t_{aei}) \quad (25)$$

$$\frac{dW}{dh_a} = \frac{Le(h_a-h_{aswm})}{W-W_{swm}} + \frac{1}{h_g-2501Le} \quad (26)$$

$$W_{eo} = W_{ei} - (h_{ad}-h_{atpo})(dW/dh_a)_{wtpi} \quad (27)$$

$$t_{atpo} = \frac{(h_{atpo}-2501W_{eo})}{1 + 1.085W_{eo}} \quad (28)$$

$$U_e = \frac{1}{\frac{A_e}{A_{ti}h_i} + \frac{(1-\phi)}{h_o(A_{to}/A_f + \phi_w)} + \frac{1}{h_o}} \quad (29)$$

$$U_w = \frac{1}{\frac{b_rA_g}{h_iA_{ti}} + \frac{b_{wm}(1-\phi)}{h_w(A_{to}/A_f + \phi_w)} + \frac{b_{wm}}{h_w}} \quad (30)$$

$$b_r = \frac{h_{asr}-h_{asr}}{t_r-t_{rs}} \quad (31)$$

$$b = 0.0026(t_{as} + 10)^{1.03463} + 1.48609 \quad (32)$$

$$h_{as} = a + bt_{as} \quad (33)$$

$$h_w = \frac{1}{\frac{C_{pa}}{b_{wm}h_{ow}} + \frac{Y_w}{k_w}} \quad (34)$$

$$h_{as,m} = h_{am} - \frac{C_{pa} h_w \phi_w (1 - b_r U_w A_e)}{b_{wm} h_{ow}} \frac{(h_{am} - h_{asr})}{h_i A_{ti}} \quad (35)$$

$$h_{am} = h_{asr} + \Delta h_{am} \quad (36)$$

$$\Delta h_{am} = \frac{h_{wt} p_i - h_{wt} p_o}{\frac{\ln(h_{wt} p_i - h_{asr})}{(h_{wt} p_o - h_{asr})}} \quad (37)$$

$$t_{as} = -5.7986 + 0.656758 h_{as} - 4.502857 \times 10^{-3} h_{as}^2 + 1.53577 \times 10^{-5} h_{as}^3 \quad 0 < t_{as} < 50^\circ C \quad (38)$$

$$t_t = t_{rs} + \frac{U_w A_e (h_{am} - h_{asr})}{h_i A_{ti}} \quad (39)$$

$$\begin{aligned} q_e &= q_{tp} + q_{sh} \\ &= m_{ae} (h_{aei} - h_{atpo}) + C_r (DSH) \end{aligned} \quad (40)$$

$$t_{aeo} = t_{atpo} - C_r (DSH) / C_a \quad (41)$$

$$h_{rci} = h_{rsh} - q_e / m_r \quad (42)$$

Eq.(17) is similar to Eq.(1) and is used to solve for the number of transfer units, N_{sh} , for the superheating section of the evaporator. Note that $(t_{rsho} - t_{rs})$ is the level of superheat which must be specified as an input to the model. In order to solve for N_{sh} , the air temperature at the exit of the two-phase section, t_{atpo} , must be assumed. This value of t_{atpo} will be checked with that calculated elsewhere in the model. Upon establishing N_{sh} , the superheating and two-phase fractions are determined from Eq.(18) and Eq.(19), respectively. At this point, it is necessary to determine whether any part of the evaporator is wet. This may be accomplished by using Eq.(20) to calculate the air temperature at the location where dehumidification just begins, t_{ad} , which is used to compare with t_{atpo} calculated from Eq.(16). If t_{atpo} is less than t_{ad} , the two-phase section is partially wet or entirely wet. It can be further established whether the surface is entirely wet by comparing t_{ad} with the air temperature at the evaporator inlet, t_{aei} . If t_{aei} is less than t_{ad} , the whole surface is wet, otherwise partially wet. It is probably worth mentioning that the modelling approach for the dry evaporator is discussed by Theerakulpisut [2].

If the evaporator surface is determined to be partially wet, the dry two-phase fraction, f_{dp} , may be computed from Eq.(21) and the wet two-phase fraction, f_{wtp} , from Eq.(22). The air enthalpy at the outlet of the two-phase section, h_{awtpo} , may now be established from Eq.(23). Note that the enthalpy of air at the location where dehumidification just begins (inlet of wet two-phase section), h_{ad} is given by Eq.(24) if the evaporator is partially wet or by Eq.(25) if it is entirely wet. Eq.(26), given by Threlkeld [3], is used to calculate the change in humidity ratio with respect to the change in enthalpy when the air moves across the wet surface. The air humidity ratio at the evaporator outlet, W_{eo} , is then computed from Eq.(27) and t_{atpo} from Eq.(28). The value of t_{atpo} is then compared with the assumed value used in Eq.(17). If they do not agree within a specified tolerance, the new value is used in Eq.(17) to repeat the whole calculational procedure until the convergence criterion is satisfied.

Eqs.(29)-(39) are for the calculations of some parameters required in Eq.(20), Eq.(23) and Eq.(26). Note that the calculation of the overall heat transfer coefficient for a wet evaporator surface, U_w , requires the knowledge of tube temperature, t_t , and mean water film temperature, t_{wm} . The values of these two parameters must be initially assumed to enable the calculation of b_r , b_{wm} and h_w from Eq.(31), Eq.(32) and Eqs(34), respectively. The calculation of b_{wm} by evaluating b at the mean water film temperature is worthy of further discussion. The parameter b is defined by Eq.(33) which, over a small temperature range, linearly relates saturation enthalpy and saturation temperature of air. This equation was obtained by curve-fitting the average values of b over temperature intervals of 5°C as a function of the air saturation temperature corresponding to the mid-point of each interval. After evaluating b_r , b_{wm} and h_w , U_w is calculated. The new value of t_t is then established from Eq.(39) and compared with the assumed value. If they do not agree within aspecified limit, the new value is used to replace the old value in evaluating U_w until agreement is achieved. The assumed value of t_{wm} can be checked by using Eq.(35) to evaluate h_{aswm} which is used in Eq.(38) to compute t_{wm} . The new t_{wm} is then compared with the assumed value. If they do not agree within a specified tolerance, the new value is used to repeat the calculational process until agreement is achieved.

The cooling load of the evaporator may be calculated by Eq.(40). The air temperature at the outlet of the evaporator is given in Eq.(41) whereas the air humidity ratio at this location is taken as W_{eo} . The refrigerant enthalpy at the inlet of the evaporator, h_{rei} may be established by Eq.(42). With the knowledge of h_{rei} and the refrigerant pressure, the refrigerant state at the evaporator inlet is fixed.

COMPRESSOR MODEL

Like most compressor models of refrigerating compressors, the compressor model in this study makes use of a perfect gas simulation utilizing a polytropic process in order to limit the required computer time by using a reasonably compact formulation of the governing equations.

Threlkeld [3] has derived the relationships for the volumetric efficiency and the theoretical work input per unit mass of refrigerant of a reciprocating compressor to be

$$\eta_v = [1 + C - C(P_c/P_b)^{1/n}](v_4/v_b) \quad (43)$$

$$W = \frac{n}{n-1} P_b v_b [(P_c/P_b)^{(n-1)/n} - 1] \quad (44)$$

From the basic definition of volumetric efficiency,

$$\eta_v = m_r v_4 / P D \quad (45)$$

it follows that

$$m_r = [1 + C - C(P_b/P_c)](P D / v_b) \quad (46)$$

By introducing the motor efficiency, η_{mot} , and compressor efficiency, η_{mech} , the actual power input required by the compressor may be written as

$$W_{act} = m_r W / (\eta_{mot} \eta_{mech}) \quad (47)$$

Eqs.(43)-(47) form the basis of the compressor model.

THERMOSTATIC EXPANSION MODEL

The principal task of the evaporator model is the prediction of the refrigerant mass flow rate for a given net pressure drop across the valve. For a given thermostatic expansion valve, the best approach is to define the model using a curve-fitting technique on the manufacturer's data. The form of the equation used by most researchers follows from the standard orifice equation which describes the mass flow rate as the square root of pressure drop times a constant.

$$m_r = C_{tx} (\Delta T_o - \Delta T_s) (\rho_l \Delta P_{tg})^{1/2} \quad (48)$$

The flow coefficient, C_{tx} , must be established from the manufacturer's data. Note that ΔP_{tg} is $P_1 - P_2$ and that P_1 and P_2 may be respectively expressed as functions of P_c and P_b by taking into account the high side and low side pressure losses. By equating Eq.(46) and Eq.(48), P_c may be established for any given value of P_b .

PRESSURE DROP AND CALCULATIONS

The analysis of pressure drops in the heat pump circuit involves the computation of both single-phase and two-phase pressure drops. Pressure losses in fluid flow are attributable to three basic phenomena, namely, acceleration, friction and gravity. Calculations of these pressure losses are based on correlations by a number of researchers. Because of the tedious and lengthy nature of the calculational procedures involved, the pressure drop calculations will not be further discussed here. Interested readers are referred to the Ph.D.thesis by Theerakulpisut [2] for further details.

OTHER MINOR COMPONENT MODELS

Besides the component models just outlined, the heat pump model also requires other minor models such as air mixing model, compressor suction line model, compressor discharge line model and liquid line model. These minor components are simple to model and will not be discussed here. It is however worth mentioning that the air mixing model is assumed to be adiabatic. The suction line, discharge line and liquid line models take account of the heat gain by or loss from the lines.

Also, it should be noted that some of the parameters previously presented such as convective heat transfer coefficients on the air side and refrigerant side, properties of air and refrigerant, and efficiency of dry and wet fins, are necessarily left out in this presentation. Some of these parameters require lengthy discussion and computational procedure due to complexity of the actual processes involved.

MODEL VERIFICATION

A heat pump experimental rig was constructed for model verification. The experimental rig was installed with measuring equipment capable of continuous monitoring of important parameters such as evaporator exit air temperature and humidity ratio, condenser exit air temperature, heating capacity, compressor power input, coefficient of performance, suction pressure, discharge pressure and refrigerant mass flow rate. Comparison between simulation results and experimental data are presented in Figure 4 - Figure 12. From these figures, it can be concluded that the simulation and experimental results match very well.

DISCUSSIONS AND CONCLUSIONS

The heat pump model has briefly been outlined with necessary details to cover the basic structures of component models. The model was simulated and verified by experimental results to be highly accurate. The simulation and experimental results indicate that the heat pump model is highly accurate and suitable for use in a heat pump drying study as intended.

REFERENCES

1. Kreider, J.F., and Kreith, F. (1981). *Solar Energy Handbook*. McGraw-Hill Book Company.
2. Theerakulpisut, S. (1990). *Modelling Heat Pump Grain Drying Systems*. Ph.D. Thesis, University of Melbourne, Australia.
3. Threlkeld, J.L. (1972). *Thermal Environmental Engineering*. Prentice-Hall, Inc.

Nomenclature

The symbols used in this paper are listed below for reference.

A	=	area (m^2)
b	=	parameter defined by Eq. (33)
b_r	=	parameter defined by Eq. (31)
C	=	capacity rate (kW/K)
C	=	clearance factor (dimensionless)
C_p	=	specific heat of fluid (kJ/kg/K)
h	=	enthalpy of fluid (kJ/kg)
h	=	convective heat transfer coefficient (kW/m ² /K)
h_{fg}	=	vaporization enthalpy of water (J/kg or kJ/kg)
k	=	thermal conductivity (kW/m/K)
Le	=	Lewis number (dimensionless)
m	=	mass flow rate (kg/s)
N	=	number of transfer units (dimensionless)
N_u	=	Nusselt number (dimensionless)
n	=	compression index (Dimensionless)
P	=	pressure (kPa)
ΔP	=	pressure drop (kPa)
PD	=	piston displacement (m ³ /s)
q	=	heat transfer rate (kW)
T	=	temperature (C or K)

t	=	temperature (C or K)
U	=	overall heat transfer coefficient ($\text{kW/m}^2/\text{K}$)
U_w	=	overall heat transfer coefficient of wet surface based on enthalpy difference ($\text{kg/m}^2/\text{s}$)
W	=	humidity ratio (kg water/kg dry air)
W	=	theoretical work input per unit mass of refrigerant (kJ/kg)
x	=	refrigerant quality (dimensionless)
y_w	=	thickness of water film (m)

Greek symbols

ϵ	=	heat exchanger effectiveness (dimensionless)
η_v	=	volumetric efficiency (in decimal form)
η_{mot}	=	motor efficiency (in decimal form)
η_{mech}	=	compressor mechanical efficiency (in decimal form)
	=	density (kg/m^3)

Subscripts

a	=	air
c	=	condenser
d	=	dew point
e	=	evaporator
dsh	=	desuperheating
f	=	fin
i	=	inlet, inside
o	=	outlet, outside
r	=	refrigerant
s	=	saturation
sc	=	subcooled
sh	=	superheating
t	=	tube
tp	=	two-phase

Note that these subscripts are also used in combination. For example, t_{rpi} refers to refrigerant temperature at the inlet of two-phase section.

Figure 4 : Predicted VS Experimental
Evaporator Exit Air Humidity Ratio

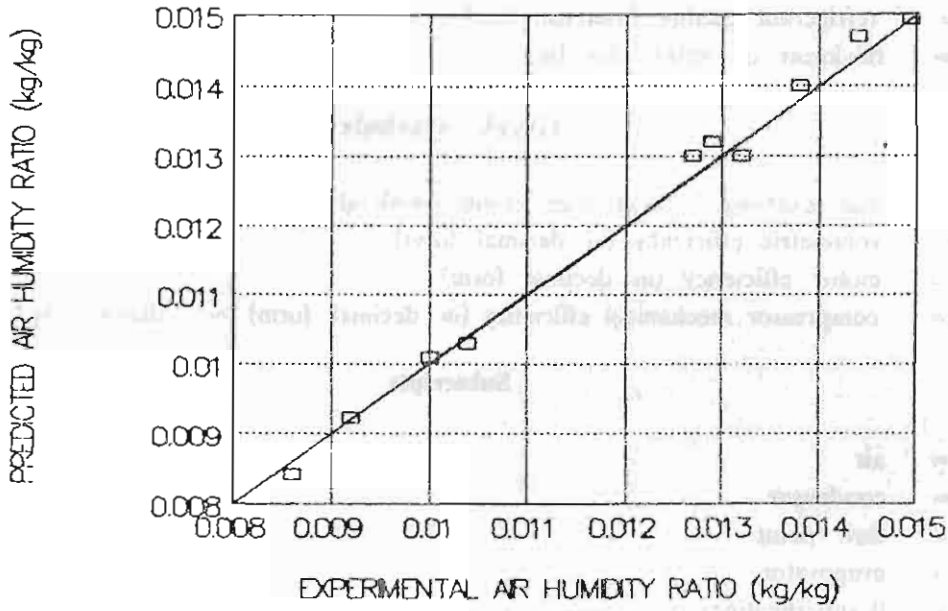


Figure 5 : Predicted VS Experimental
Evaporator Exit Air Temperatures

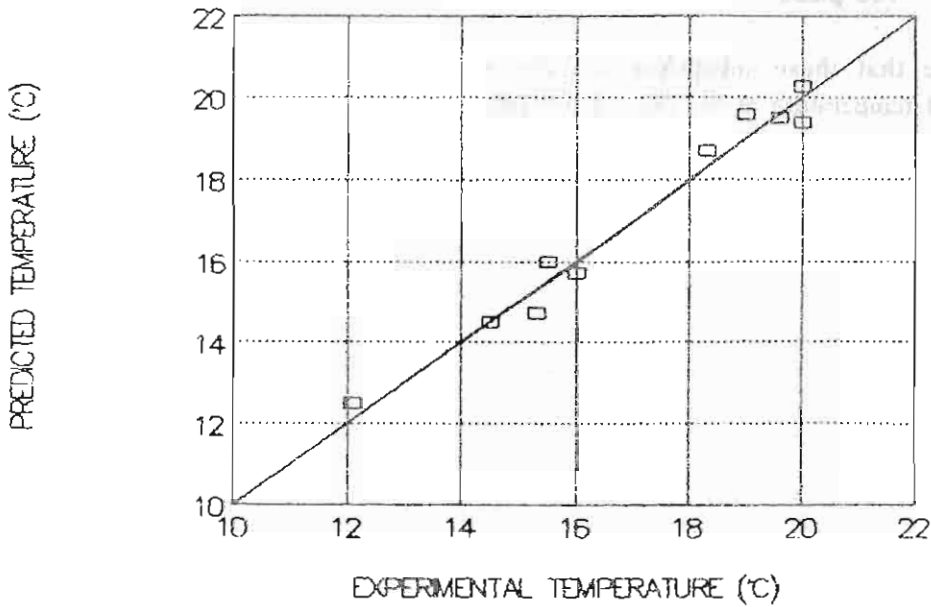


Figure 8 : Predicted VS Experimental

Compressor Power Inputs

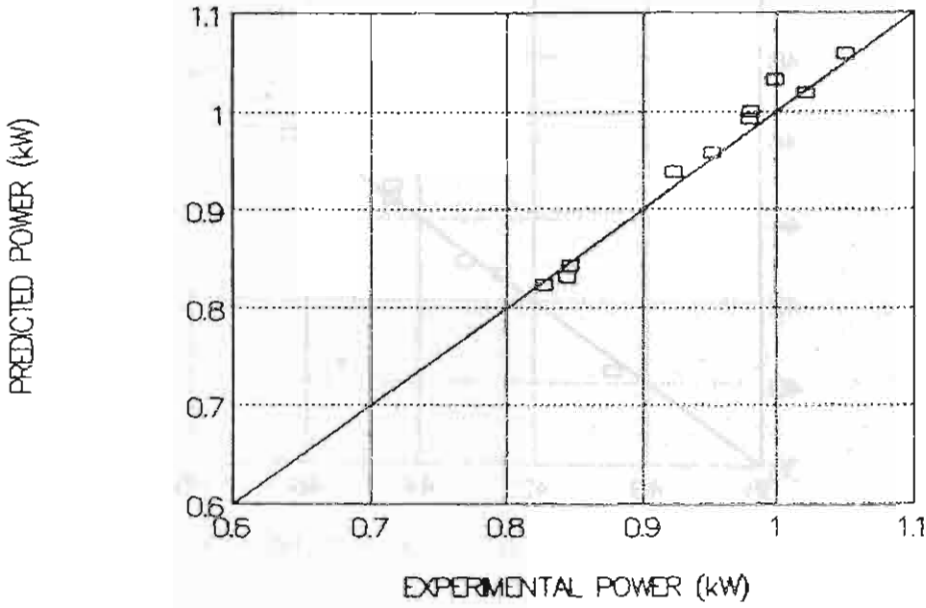


Figure 9 : Predicted VS Experimental

Coefficients of Performance

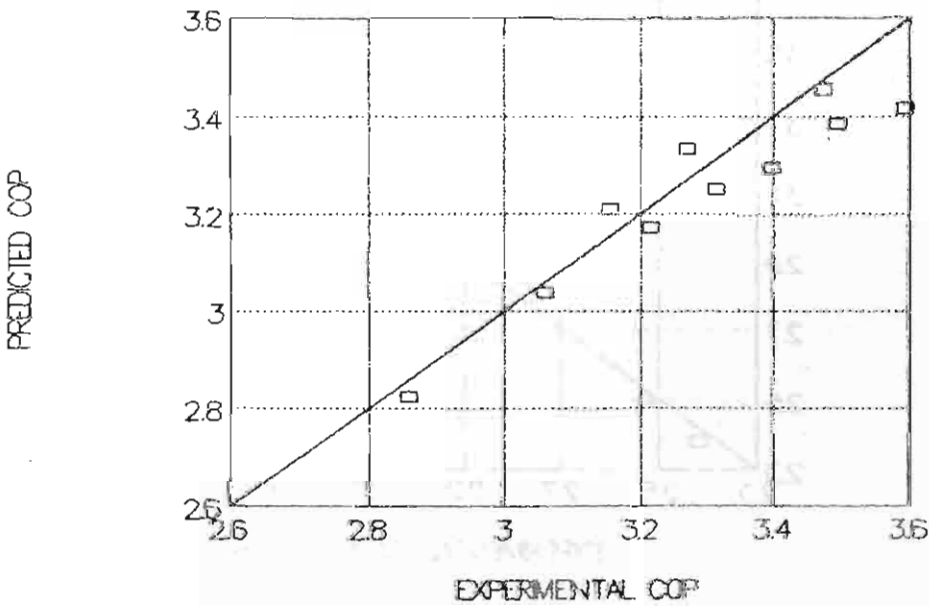


Figure 10 : Predicted VS Experimental

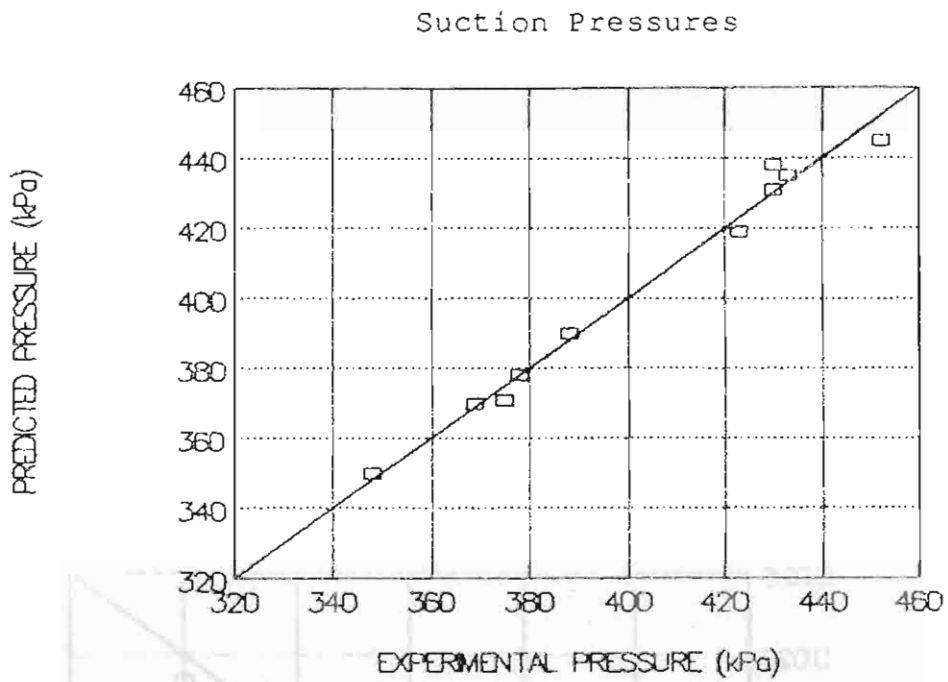


Figure 11 : Predicted VS Experimental

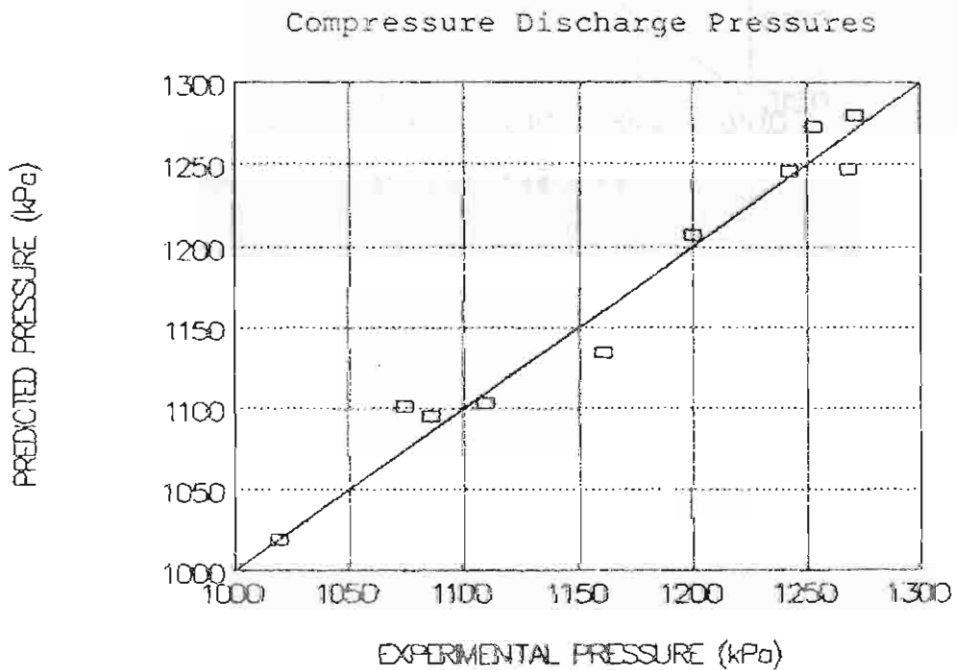


Figure 12 : Predicted VS Experimental
Refrigerant Mass Flow Rates

